ORNL/TM-2018/929

# *Complete Status Report Documenting the Development of Friction Stir Welding for Producing a Butt Joint in Thin Wall Tubing of ODS Alloys*

**Nuclear Technology Research and Development**

***Prepared for***
***U.S. Department of Energy***
***Nuclear Technology R&D***
***Advanced Fuels Campaign***

***David T. Hoelzer, Caleb P. Massey***
***Christopher M. Fancher and Wei Tang***

***Oak Ridge National Laboratory***

***September 21, 2018***
**M3NT-18OR020302041**

**CONTENTS**

**Page**

## LIST OF FIGURES

## ACKNOWLEDGMENTS

This research was sponsored by the U.S. Department of Energy, Office of Nuclear Energy, for the Nuclear Technology Research and Development (NTRD) program.

The authors are grateful to Tom Geer for assistance in preparation of the metallographic sample of the 1.0 mm thick plate containing the butt joint produced by friction stir welding and his assistance with optical microscopy. The authors want to also acknowledge Yukinori Yamamoto and Boopathy Kambaiah for reviewing the manuscript.

**ABSTRACT**

A challenging attempt using friction stir welding to produce a butt joint between two 1.0 mm thick plates of 14YWT was nearly successful. The modified tool pin mostly penetrated the thickness of the adjoined thin plate samples resulting in a small blunt notch on the bottom surface of the butt joint. A bend occurred in the thin plate sample due to formation of stresses from clamping the thin plate sample during FSW. The peak displacement of the bend occurred along the center line of the butt joint. The weld zone showed good microstructure mixing with some flashing mostly on the retreating side that suggested excess heat input by friction between the traveling and spinning tool pin and thin plates of 14YWT.

Neutron diffraction experiments were performed on the bent sample of 14YWT to measure the residual stresses in the butt joint on the HB-2B beam line at the Neutron Residual Stress Facility at HFIR. However, the neutron scattering to background noise ratio was very low during data acquisition. Measurements of lattice strains were obtained in the rolling (RD) and normal (ND) directions but not in the extrusion direction (ED) of the thin plate sample. Unfortunately, the quality of the data was not sufficient for determining the residual stresses in the butt joint. From the previous neutron scattering experiments conducted on four hot rolled plates (R1, R2, R3 and R4) of 14YWT, the residual stresses were calculated from lattice strain data and plotted in 2-D color contour maps for ED, RD and ND. The results showed variations in the magnitude and spatial position of residual stresses in the microstructure of the four plates. The magnitude in residual stresses in ED and RD increased gradually with increasing rolling deformation for R1 (50%) to R2 (76%), followed by larger increases in R3 (89%) and R4 (95%). The maximum peaks in residual stresses for R4 was ~710-730 MPa in ED and RD. The residual stresses in ND were below ~300 MPa for each of the 4 rolled plates, with a maximum residual stress in R4 (95%) of ~400 MPa. These results indicated that significant residual stresses representing ~57% of the yield stress of 14YWT (SM13) had accumulated in the 14YWT plate after hot rolling to the 1 mm thickness, which was used in the FSW experiments.

The microstructure analysis of the 1.0 mm thick plate of 14YWT containing the butt joint produced by FSW revealed significant changes in the grain structure and texture between the unaffected zone (UZ) of the rolled plate and the butt joint weld. In the UZ, the grains were severely elongated after 95% deformation and mainly possessed the {101} texture component in the ED. Two predominant grain misorientation angles were observed: one consisting of small misorientations of <5º between highly elongated grains and the other consisting of large misorientations of >15º in pockets of small grains that might have formed by dynamic recrystallization processes during rolling of the plate at 1000ºC. The morphology and texture of grains in the heat affected zone (HAZ) were similar to those in UZ, except the grains had coarsened due to excess heat input during FSZ. A population of pores formed and the grains both coarsened and changed to isotropic morphology in the microstructure of the butt joint on both the advancing and retreating sides. The texture of grains in both regions were randomly orientated between the 3 poles {001}, {101} and {111}. The main difference in texture of grains between the advancing side and retreating side was with the misorientation angles of neighboring grains. Most of the grains in the advancing side had misorientation angles of >5º indicating that these grains experienced recrystallization. On the retreating side, areas containing larger grains showed high misorientation angles of >15º compared to areas appearing as bands of grains with misorientation angles of <5º and between 5º-15º. Numerous small pockets of grains with low misorientation angles of <5º were distributed in the microstructure among the grains showing high misorientation angles of >15º. It was determined that the grains associated with low misorientation angles contained sub-grain structures, which was consistent with both recrystallization and recovery mechanisms for grains located on the retreating side of the butt joint. These results demonstrate the complex microstructure that evolves in the microstructure of 14YWT resulting from the input of high temperatures and severe deformations during FSW.

.

## 1. INTRODUCTION

The joining of the advanced ODS 14YTW ferritic alloy presents a significant challenge since the carefully tailored microstructure containing ultra-small grains and a high concentration of nano-size oxide particles, or nanoclusters, must be preserved with little to no degradation in high-temperature mechanical properties and radiation tolerance. Friction stir welding (FSW) is a solid-state joining technique that has the potential of not disrupting the salient microstructure features of 14YWT. For this reason, FSW is being investigated in the NTRD program with the goal of joining thin wall fuel cladding of 14YWT for fast nuclear reactor technologies. However, to achieve this goal, the FSW conditions must be developed for joining plate and tubing of 14YWT that are <1.0 mm thick.

In past research, the first FSW experiment successfully produced a bead-on-plate stir zone (SZ) on the 1.0 mm thick plate of 14YWT. Microstructure characterization studies of the stir zone (SZ) showed that the grain structure increased slightly in size and was isotropic in shape compared to the highly elongated grains observed in the base metal (BM) and that the nano-size Y-Ti-O oxide particles exhibited slight coarsening in size. Several cracks oriented horizontally to the plane of the 1.0 mm thick plate were observed in the SZ, thermal mechanically affected zone (TMAZ) and BM on the retreating side of the weld that may have formed by the combination of stresses introduced by clamping of the plate during FSW and residual stresses from deformation rolling of the 1.0 mm thick plate and from FSW in the SZ. The tensile properties and plastic deformation behavior of the SZ and base metal (BM) were investigated using digital image correlation (DIC) during in-situ tensile testing of miniature tensile specimens to assess the quality of the FSW parameters. The results of the DIC analysis of the tensile tested miniature specimens showed that the strength properties of specimens from the SZ decreased ~13% compared to specimens from the BM, but that the ductility properties were essentially unchanged by FSW. All specimens exhibited similar deformation behavior that consisted of increased intensity of strain localization and local strain rates in the region of the specimen gauge where necking occurred until the specimen failed. The results suggested that deformation bands may be slightly more prevalent during deformation in specimens from the stir zone compared to the unaffected zone.

It was reported in the FY17 milestone (M3FT-17OR020302031) that hot rolling plates of 14YWT at 1000ºC from 10 mm to 1.0 mm thickness resulted in the accumulation of residual strains that increased with rolling deformation magnitude. The dependence of the residual strains on orientation within the hot rolled plates was obtained by scanning each plate in the extrusion direction (ED), rolling direction (RD), which was perpendicular to ED, and normal direction (ND) to the surface of the rolled plates. The results indicated that residuals strains increased in ED and RD with increasing deformation magnitude but were insensitive to the deformation magnitude in ND. This observation was consistent with deformation occurring in plane in the plates during rolling. In this report, the residual stresses were calculated from the residual strains and plotted in 2-D contour maps to show the spatial distribution and magnitude of residual stresses caused by rolling. Additional residual stress measurements were conducted in a new ORNL Neutron Science User proposal that was awarded beam time at the Neutron Residual Stress Facility at HFIR to determine the magnitude and orientation dependence of residual stresses in a butt joint produced by FSW. The microstructure of the butt joint and surrounding 14YWT plate was investigated to correlate with FSW parameters and residual stress measurements.

## 2. MATERIALS AND EXPERIMENTAL

### *2.1. Friction stir welding*

As reported in milestone M3FT-17OR020302031, a 10 mm thick plate of 14YWT was rolled at 1000ºC to a final thickness of 1.0 mm with plates of 5 mm and 2.2 mm thickness retained for residual stress measurements. Figure 1 shows the 1.0 mm thick plate and the orientation of the extrusion and rolling

directions. This plate was cut in half along the white dash line. The sample on the left side of the cut was used for producing a bead-on-plate weld zone by friction stir welding (FSW).

In this report, the sample on the right side of the cut in the 1.0 mm thick plate of 14YWT was used for producing a butt joint by FSW. This sample was cut into two halves along the yellow dash line observed in Figure 1. This orientation in cut resulted in two halves with similar thicknesses along the edges for improving the butt joint quality.

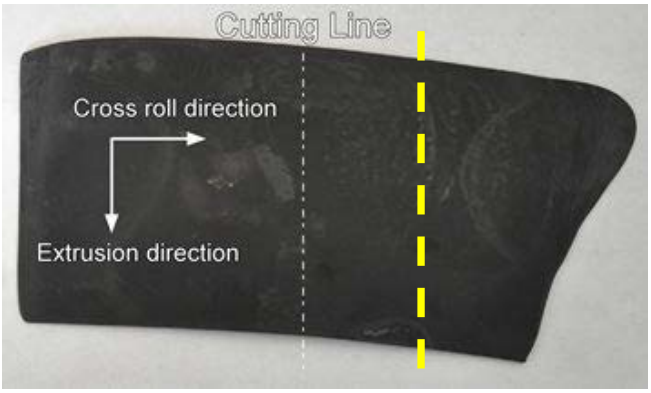


Figure 1. Optical image showing the layout of the samples cut from the 1.0 mm thick plate of 14YWT.

*2.2. Residual stress measurements*

Neutron diffraction experiments were performed on the 14YWT sample shown in Figure 2 that contained the butt joint produced by FSW. The residual stress measurements were conducted on the HB-2B beam line at the Neutron Residual Stress Facility at HFIR. This research was associated with the ORNL Neutron Science User proposal (IPTS-19909.1) titled "The Role of Friction Stir Welding on Generating Residual Stresses in a Thin Plate of 14YWT" that was awarded beam time in January 2018. The proposed research plan was to collect strain data in the form of 2-D plane of points to measure the magnitude and spatial distribution of strain in the FSW butt joint of the 1.0 mm thick plate of 14YWT. Measurements of strain were performed in the butt joint and small regions of the adjacent plate. The neutron diffraction experiments required the sample goniometer that allowed for spatial scanning of strains at different depths for determining the maximum scattering intensity from a Gaussian distribution. The scanning experiments consisted of a 2-D grid of points ($s_x$ and $s_y$) on the surface of the plate at a depth in the plate corresponding to the maximum scattering intensity ($s_z$). The {112} bcc-Fe peak was used in the neutron scanning experiments. The scans were performed in the extrusion (ED), rolling (RD) and normal (ND) directions of the samples. The strain-free lattice parameter "d-zero" value was also determined using a sample of 14YWT that was annealed at 1000ºC for 30 min. in vacuum followed by slow cooling in the furnace to reduce residual stresses from hot-rolling. Overall, enough neutron counts were obtained from the RD and ND orientations, but the neutron scattering signal-to-background noise (i.e. neutrons) was too small for the ED orientation.

*2.3. Microstructure analysis*

A specimen containing a cross-section of the butt joint weld zone in the 1.0 mm thick plate of 14YWT was prepared for scanning electron microscopy (SEM) analysis. During cutting using a diamond impregnated tip blade, the specimen broke along the center of the butt joint. The two halves of the specimen were mounted in epoxy and metallographically prepared with a final polishing using colloidal silica (0.05 μm). The polished specimens were examined using a Hitachi 4800 field emission scanning electron microscope (FE SEM) equipped with X-ray energy dispersive spectroscopy (XEDS). The collected microstructural

information included secondary electron (SE) and backscattered electron (BSE) imaging and electron backscattered diffraction (EBSD) for obtaining details about grain morphology, porosity, oxide particle coarsening and texture induced by rolling to produce the 1.0 mm thick plate of 14YWT and FSW to produce the butt joint. The EBSD data was collected using a 20kV accelerating voltage with a 4nA tip current.

## 3. RESULTS AND DISCUSSION

### *3.1 Friction stir welding*

Figure 2 shows the butt joint weld zone that was produced by FSW. Special precautions were taken to clamp the two samples of the 1.0 mm thick plates of 14YWT to minimize bending stresses that may occur during the FSW run. Figure 2a shows the view normal to the butt joint with labels showing the advancing and retreating sides and the clockwise rotation of the tool pin as it traveled in the advancing direction. The tool pin did not fully penetrate the butt joint, but was very close to penetrating. This resulted in a small but blunt notch between adjacent sample edges on the bottom surface of the butt joint weld. From optical inspection, the weld zone showed good microstructure mixing. Some flashing mostly on the retreating side occurred that was possibly due to excessive heat input by friction between the traveling and spinning tool pin and adjacent thin plates of 14YWT. It was also observed that the thin plate sample was bent after the FSW run was completed and the clamping was released. This bend is observed with the oblique view of the thin plate of 14YWT shown in Figure 2b. The black dash line superimposed on the image shows that the peak displacement of the bend occurred along the center line of the butt joint. This observation most likely caused by residual stresses that formed during FSW of the clamped thin plate samples of 14YWT.

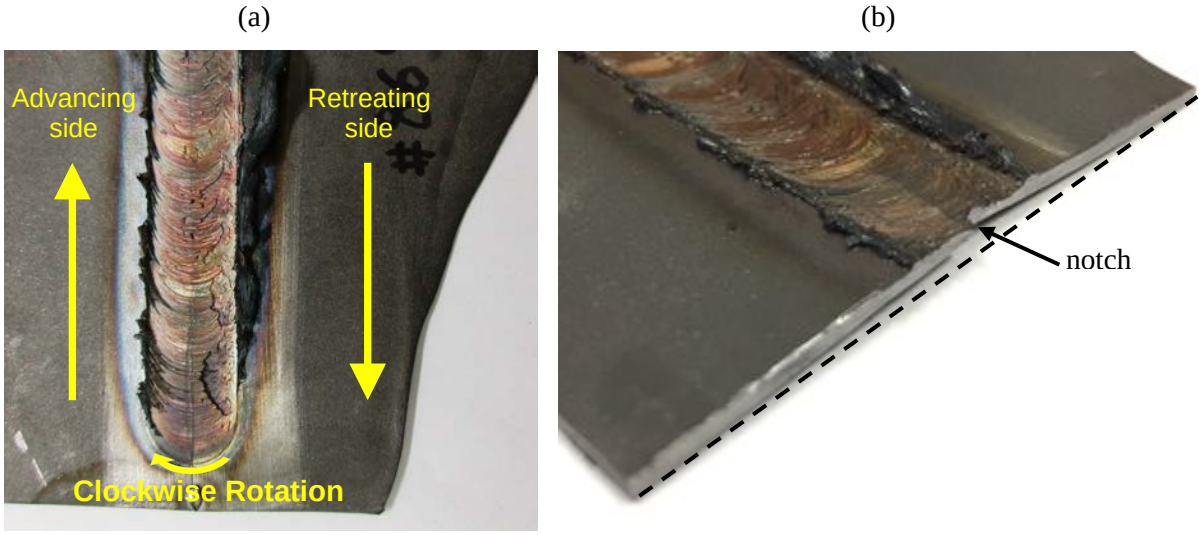


Figure 2. Optical images showing the butt joint weld zone produced by FSW between two halves of the 1.0 mm thick plates of 14YWT. (a) Viewed normal to the butt joint and (b) viewed at an oblique view of the butt joint.

### *3.2 Residual stress measurements*

In milestone M3FT-17OR020302031, the residual strains were reported from neutron diffraction experiments conducted on four plates of 14YWT (SM13 heat) that were rolled from the starting thickness of 10 mm (R1 plate; 50% reduction in thickness) to the final thickness of 1.0 mm (R4 plate), which was used in FSW experiment. Figure 3 shows images of plates R2, R3 and R4 after being rolled to thicknesses of 5 mm (Fig. 3a), 2.2 mm (Fig. 3b) and 1.0 mm (Fig. 3c), respectively, representing rolling deformation magnitudes corresponding to 76%, 89% and 95%, respectively. Due to differences in plate thickness that

affected the neutron scattering intensity, the residual strain measurements were obtained as 2-D grids of data points with grid sizes of 9 × 7 for R1, 11 × 8 for R2, 5 × 3 for R3 and 5 × 3 for R4, which corresponded to 63, 88, 15 and 15 number of data points, respectively. Furthermore, only the residual strains were calculated, and the 2-D data was plotted in x-y scatter plots and not as 2-D residual strain maps.

1. (a) (b) (c)

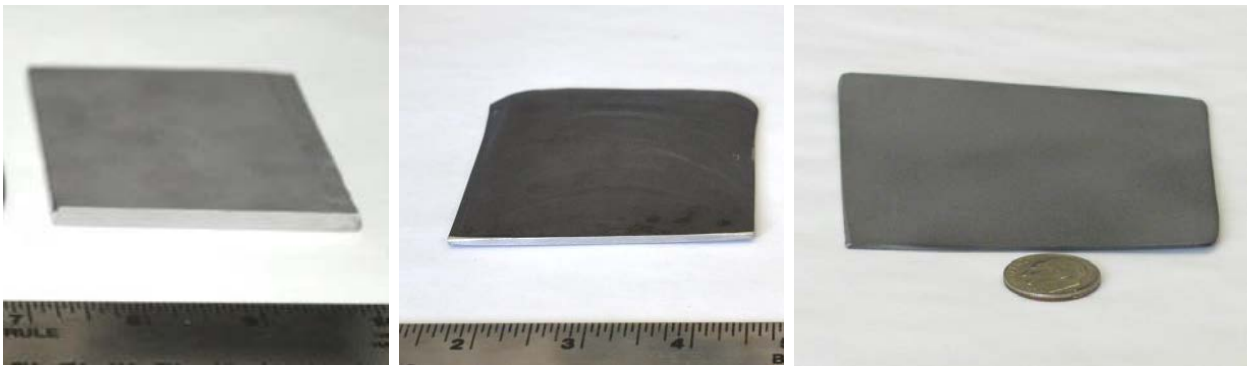

Figure 3. Digital images of the (a) 5 mm thick R2 plate, (b) 2.2. mm thick R3 plate and (c) 1.0 mm thick R4 plate of 14YWT-SM13.

The residual strains obtained from neutron scattering were measured for $\{112\}_{hkl}$ peaks. The d-spacing of the {112} planes were determined from the neutron scattering data and used in calculating the lattice strain using the following equation:

$$\varepsilon = \frac{d_{hkl} - d_0}{d_0}$$

where, $d_{hkl}$ is the measured d-spacing of {112} from the scattering experiments and $d_0$ is the reference d-spacing of {112} usually obtained from an unstrained sample. Thus, the lattice strain is due to the change in {hkl} peak position from the stress-free location in sample. In this experiment, a stress-free sample was not used. Since the stress-state is constant in each rolled plate, a stress-free region could not be used either. For this report, the reference $d_0$ was calculated from the average d-spacing of {112} planes in the R1 plate since this plate had the lowest deformation magnitude. Therefore, the calculated values of residual strains and ultimately residual stresses will underestimate the actual values.

The estimate of the residual stresses was determined from the residual strains using the Hooke's law for based on three orthogonal strain values ($\varepsilon_{11}$, $\varepsilon_{22}$ and $\varepsilon_{33}$) pertaining to the principal stress directions for ED, RD and ND:

$$\sigma_{11} = \frac{E^{hkl}}{(1-v^{hkl})(1-2v^{hkl})} \times \{\varepsilon_{11}(1-v^{hkl}) + v^{hkl}(\varepsilon_{22}+\varepsilon_{33})\}$$

where $E^{hkl}$ is the Young's Modulus, $v^{hkl}$ is the Poisson's Ratio and $\varepsilon_{ii}$ is the measured lattice strain in each direction in the plate. Values of $E^{hkl}$ and $v^{hkl}$ were recently obtained for 14YWT-SM13 by in-situ uniaxial tensile tests with high-energy synchrotron X-ray diffraction experiments at the 1-ID beamline at the Advanced Photon Source at Argonne National Laboratory [1]. At room temperature, the value for $E^{hkl}$ was ~207 GPa and for $v^{hkl}$ was ~0.20. The principal strains are $\varepsilon_{ii}$, but in this work the lattice strains are taken as the extrusion direction for $\varepsilon_{11}$, the normal direction for $\varepsilon_{22}$ and the rolling direction for $\varepsilon_{33}$.

The x-y grid of residual stress values obtained from the 4 rolled plates of 14YWT were plotted as 2-D contour maps using Origin 2018. Figures 4, 5 and 6 show the 2-D contour maps of residual stresses calculated for the R1, R2, R3 and R4 plates of 14YWT in the extrusion (ED), rolling (RD) and normal (ND) directions, respectively. The data was processed by truncating regions of the microstructures that contained compressive stresses and plotting only positive values of residual stresses for comparison between the four rolled plates. The color of the 2-D contour maps ranged from dark blue (0 MPa) to bright red (1000 MPa or higher) with black representing regions of compressive stresses. The intervals of residual stresses were set at 30 levels for R1 and at 15 levels for R2, R3 and R4 since the values of residual stresses varied over larger ranges in the latter 3 plates compared to those of R1. A few data points surpassed 1000 MPa, but were regarded as meaningless values since they typically were higher than the yield stress of 14YWT (SM13), which is ~1280 MPa at room temperature. These anomalous values may be due to neutron scattering errors in beam alignment or other artefacts not fully understood.

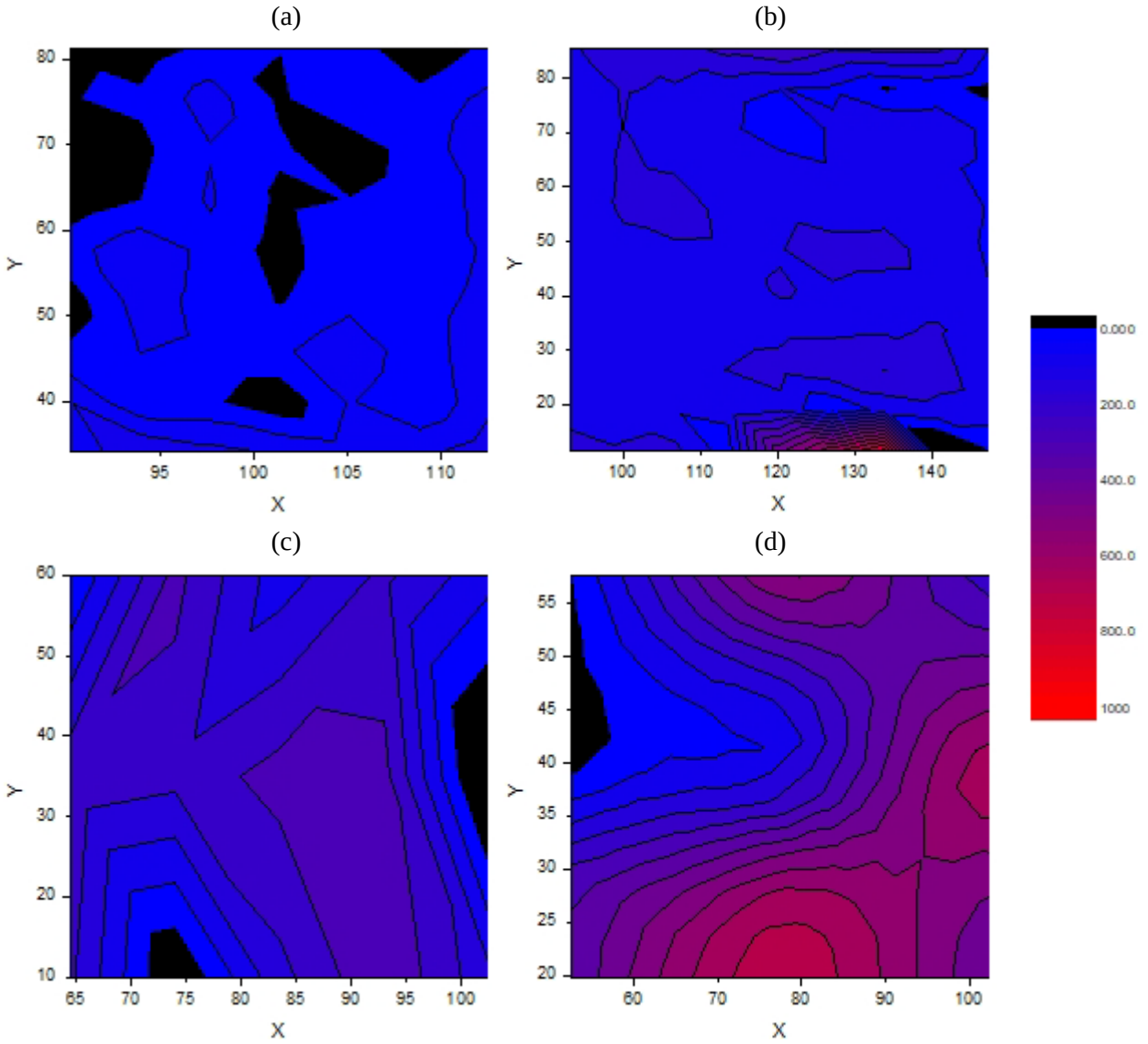


Figure 4. 2-D contour maps showing the residual stresses in the extrusion direction of plates: (a) R1, (b) R2, (c) R3 and (d) R4. Intensity scale in MPa.

The results showed that the residual stresses varied in magnitude with spatial position in the microstructure of the four plates. The magnitude in residual stresses increased gradually from plates R1 (10 mm thick) to R2 (5 mm thick), followed by larger increases in R3 (2.2 mm thick) and R4 (1.0 mm thick) with increased rolling deformation in the ED (Fig. 4) and RD (Fig. 5) directions. The largest peaks in residual stresses occurred in the R4 plate by reaching magnitudes of ~710-730 MPa in the ED (Fig. 4d) and RD (Fig. 5d) orientations. The levels of residual stresses were lower for the ND orientation compared to ED and RD. In general, the residual stresses in ND were below ~300 MPa for each of the 4 rolled plates (Fig. 6). Only in the R4 plate was a region with a residual stress of ~400 MPa measured (Fig. 6d). These results indicated that significant residual stresses representing ~57% of the yield stress of 14YWT (SM13) had accumulated in the 14YWT plate after hot rolling to the 1 mm thickness, which was used in the FSW experiments.

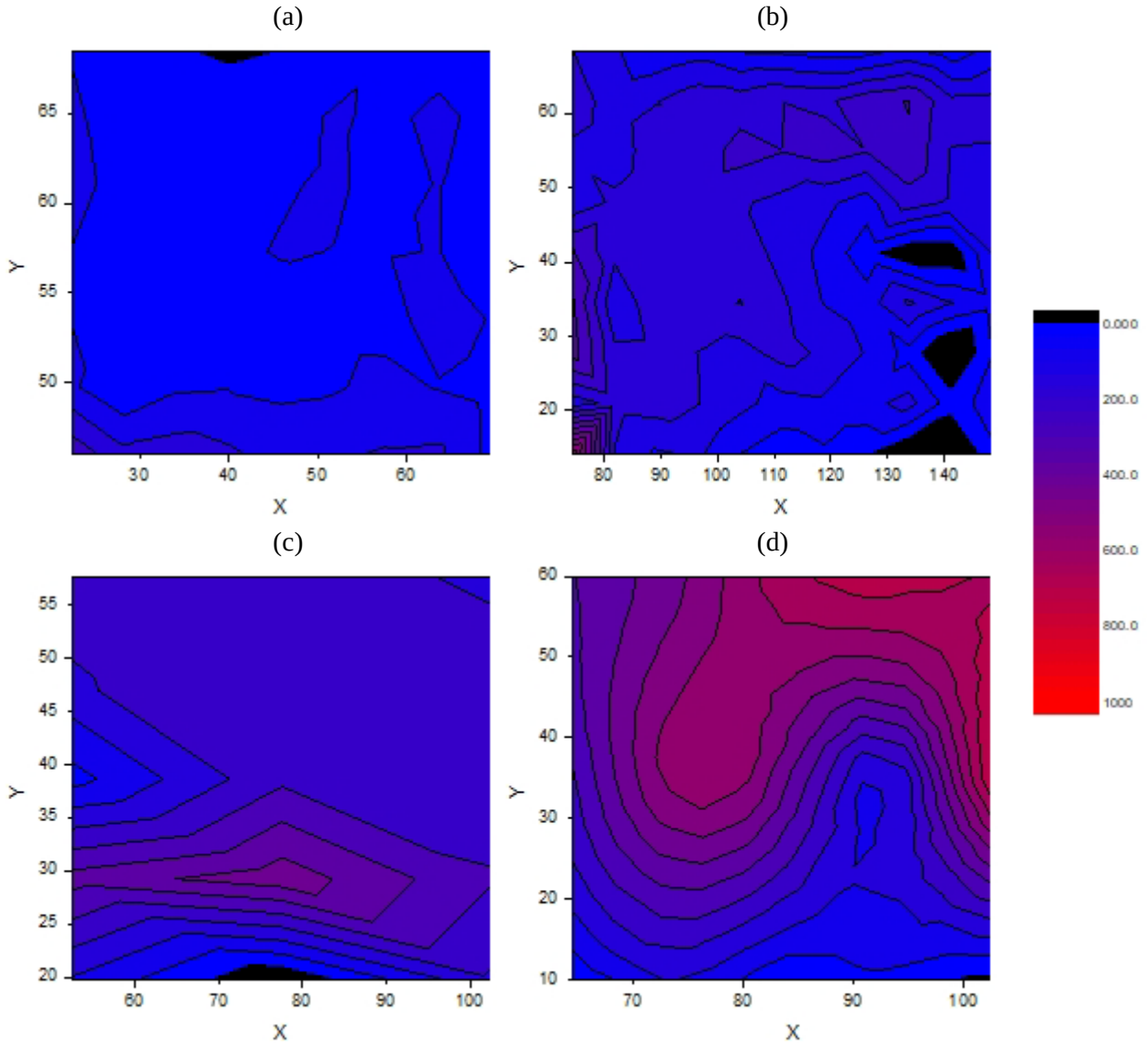


Figure 5. 2-D contour maps showing the residual stresses in the rolling direction of plates: (a) R1, (b) R2, (c) R3 and (d) R4. Intensity scale in MPa.

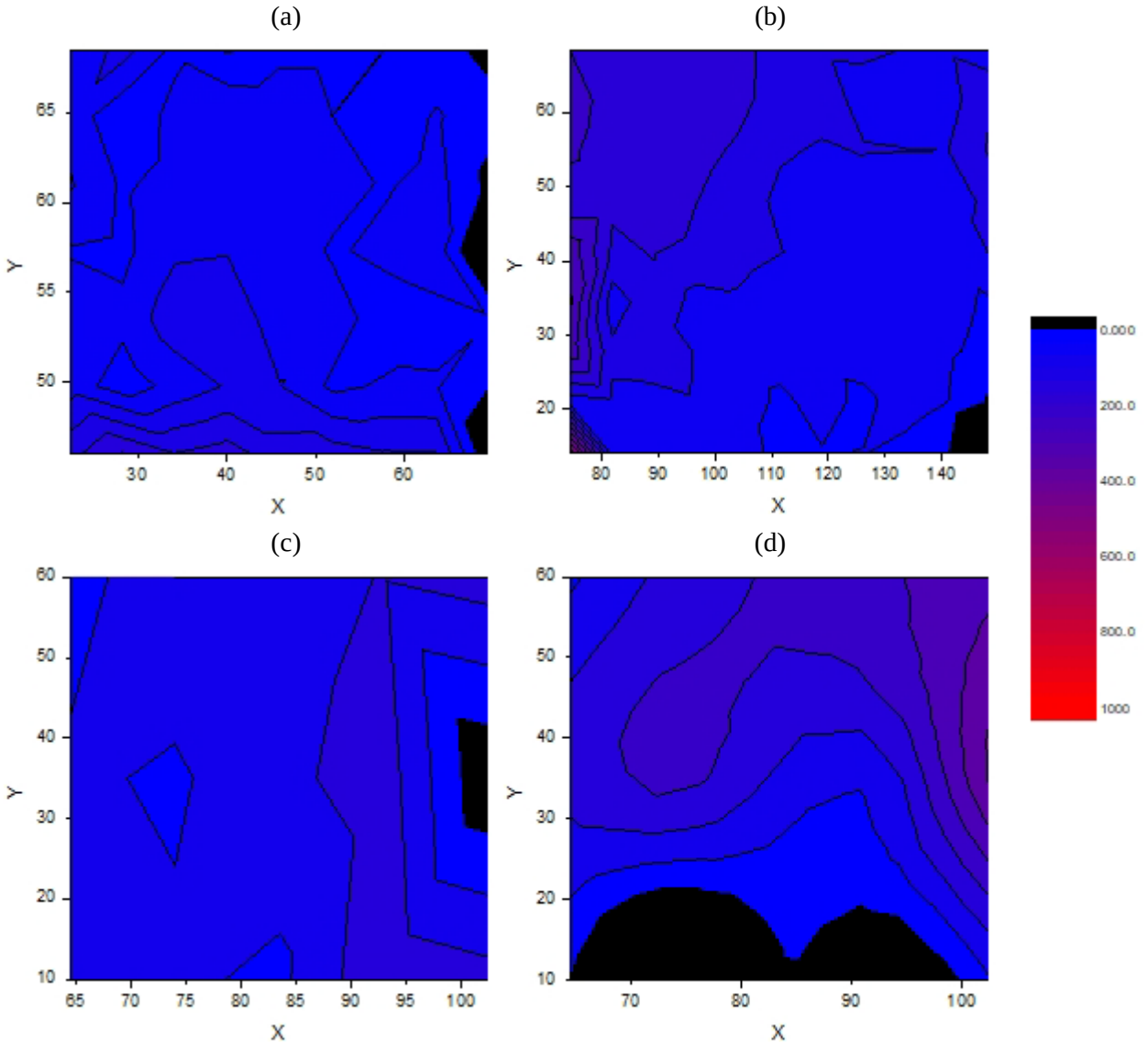


Figure 6. 2-D contour maps showing the residual stresses in the normal direction of plates: (a) R1, (b) R2, (c) R3 and (d) R4. Intensity scale in MPa.

Neutron diffraction experiments were performed to measure the lattice strains for calculating residual stresses in the butt joint of the bent 1.0 mm thick plate 14YWT on the HB-2B beam line at the Neutron Residual Stress Facility at HFIR. During the scattering experiments, it was determined that the neutron scattering to background noise ratio was very low for data acquisition. Scattering signals for the {112} lattice planes were weak and could only be measured in the RD and ND orientations, but not in the ED orientation. Unfortunately, the residual stresses for these two orientations could not be reliably determined. The low neutron scattering signal was due the uneven surface of the butt joint coupled with the reduction in thickness to ~0.7 mm on the advancing side of the butt joint from FSW. Scattering experiments utilizing energetic X-rays will be investigated in the future for determining the residual stresses in the butt joint,

*3.3 Microstructure analysis*

A composite of several optical micrographs showing the cross-section of the butt joint produced by FSW and adjacent thin plate of 14YWT is shown in Figure 7. The four numbered red boxes superimposed on the

image are regions of interest (ROI) that were analyzed by SEM/EBSD. As mentioned in section 2.3, the sample fractured during cutting into two halves near the center line of the butt joint. The cause of the fracture was most likely due to residual stresses coupled with the blunt notch at the bottom surface of the butt joint that was present between adjacent samples of the thin plate of 14YWT plate that were not joined by FSW. The bend that occurred in the thin plate sample after the FSW run (Fig. 2b) was completed probably meant that residual stresses were present. Cutting the cross-section sample from the end of the bent thin plate caused the release of these residual stresses, which then led to formation of the crack possibly at the blunt notch surface that propagated through the butt joint weld zone leading to fracture of the sample into two halve.

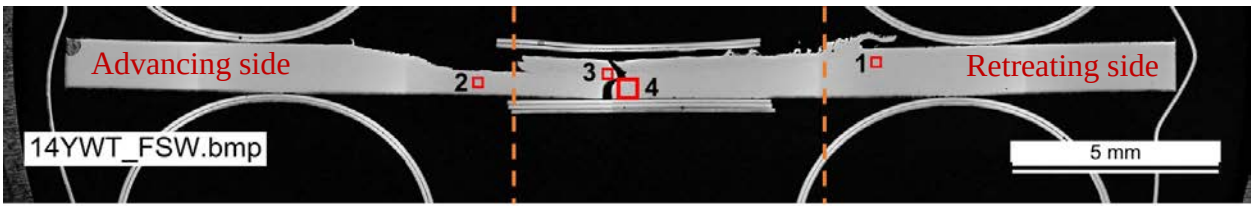


Figure 7. Composite of several optical micrographs showing the butt joint produced by friction stir welding in the 1.0 mm thick plate of 14YWT.

In Figure 7, the results showed a significant decrease in thickness of the butt joint on the advancing side compared to that on the retreating side. Flashing was also observed on the surface of the sample on the retreating side. During FSW, the rotating tool pin and shoulder was plunged with a downforce into the seam between the two thin plates of 14YWT and then translated along the seam to be joined. As the spinning tool travels along the seam, a cavity forms at the rear of the tool that is filled by redistributing and forging material of 14YWT forming the weld. The redistribution process causes severe plastic deformation and thermal exposure in the microstructure. The results observed in Figure 7 suggest that the FSW conditions caused excess heat input due to a combination of high rotation speed and downforce on the plunged tool pin and shoulder that softened the microstructure of 14YTWT [2]. This resulted in excess material of 14YWT flowing around the tool from the advancing side to the retreating side of the butt joint causing the thinner butt joint region on the advancing side.

Figure 8 shows the microstructure of 14YWT from the unaffected zone (UZ) of the 1.0 mm thick plate from ROI #1 (Fig. 7). From Figure 1, the extrusion direction in the plate lies normal to the grains observed in the micrographs. The backscattered electron (BSE) micrographs observed in Figures 8a and 8b revealed highly elongated grains and numerous blocky-shaped pores (Fig. 8a) and small particles showing dark contrast (Fig. 8b) at higher magnification. The deformation from rolling 95% reduction in thickness (RIT) was responsible for elongating the grains, which in 3-D will have pancake-type shapes. The texture of grains in revealed by EBSD is shown in Figures 8c, 8d and 8e. In Figure 8c, the insert of the inverse pole figure (IPF) in the EBSD map indicated that the grains are mostly oriented in the {101} orientation, but that components of {001} and {111} orientations also exist, as is observed in the <001> pole figure in Figure 8e (bottom). The grain internal misorientation (GIM) map of the microstructure is shown in Figure 8d along with the color representation of the misorientation angles in Figure 8e (top). Comparing the GIM map (Fig. 8d) with the EBSD map (Fig. 8c) indicated that two predominant grain misorientations were present. Grains that appeared very long in the EBSD map consisted mostly of the {101} texture that were separated by small misorientations of <5º (red) in the GIM map. On the other hand, pockets of small grains observed in the EBSD map mostly have {001} and {111} textures that were separated by large misorientations of >15ºC (blue) in the GIM map. Since the rolling of the 14YWT plate was conducted at 1000ºC, these observations suggest that the small grains with high misorientations formed by dynamic recrystallization. If this mechanism occurred, then hot rolling 14YWT at high temperatures to large deformations may be effective in modifying the strong <110>{001} texture that has been reported in cross-rolled variant of 14YWT [3].

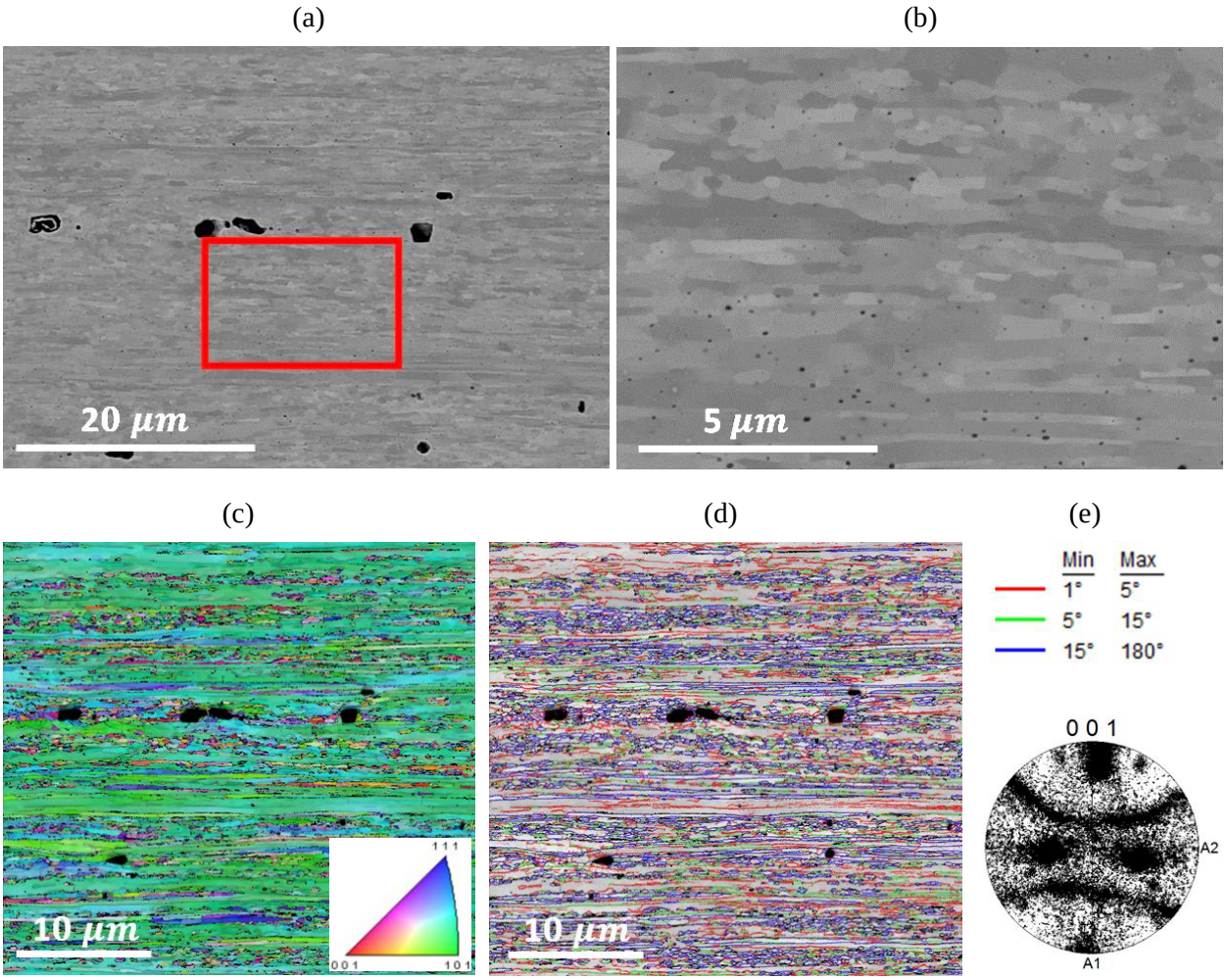


Figure 8. Showing the microstructure of the 1.0 mm thick plate of 14YWT in ROI #1 (Fig. 7). (a) and (b) BSE micrographs, (c) EBSD map and inverse pole figure (insert), (d) GIM map and (3) color indicator of GIM angles (top) and {001} pole figure (bottom).

The microstructure of the 1.0 mm thick plate of 14YWT representing the heat affected zone (HAZ) from ROI #2 (Fig. 7) is shown in Figure 9. The BSE micrographs shown in Figures 9a and 9b indicated that some of the grains appeared more isotropic in shape and coarser, while some pores (Fig. 9a) were observed as well as the small particles showing dark contrast (Fig. 9b) at higher magnification. The texture of the grains present in the HAZ of the microstructure is shown in Figures 9c, 9d and 9e. In general, the texture of the HAZ was similar to that observed in the unaffected zone of the 1.0 mm thick plate (Fig. 8). The EBSD map (Fig. 9c) and <001> pole figure (bottom in Fig. 9e) are consistent grains mostly oriented in the {101} orientation along with components of {001} and {111} orientations. The GIM map of the microstructure is shown in Figure 9d with the color index of GIM angles in Figure 9e (top). The GIM map showed most of the grains observed in the EBSD map (Fig. 9c) consisted of large misorientation angles of >15º (blue) and fewer grains with misorientation angles <5º (red). The size of the grains observed in the GIM map with high misorientation angles is larger than those observed in the GIM map of the unaffected zone (Fig. 8d). These results indicated that grains experienced coarsening mechanisms and not plastic deformation mechanisms since the grain texture was not altered significantly, which is consistent with heat affected zone associated with the butt joint in the 1.0 mm thick plate of 14YWT.

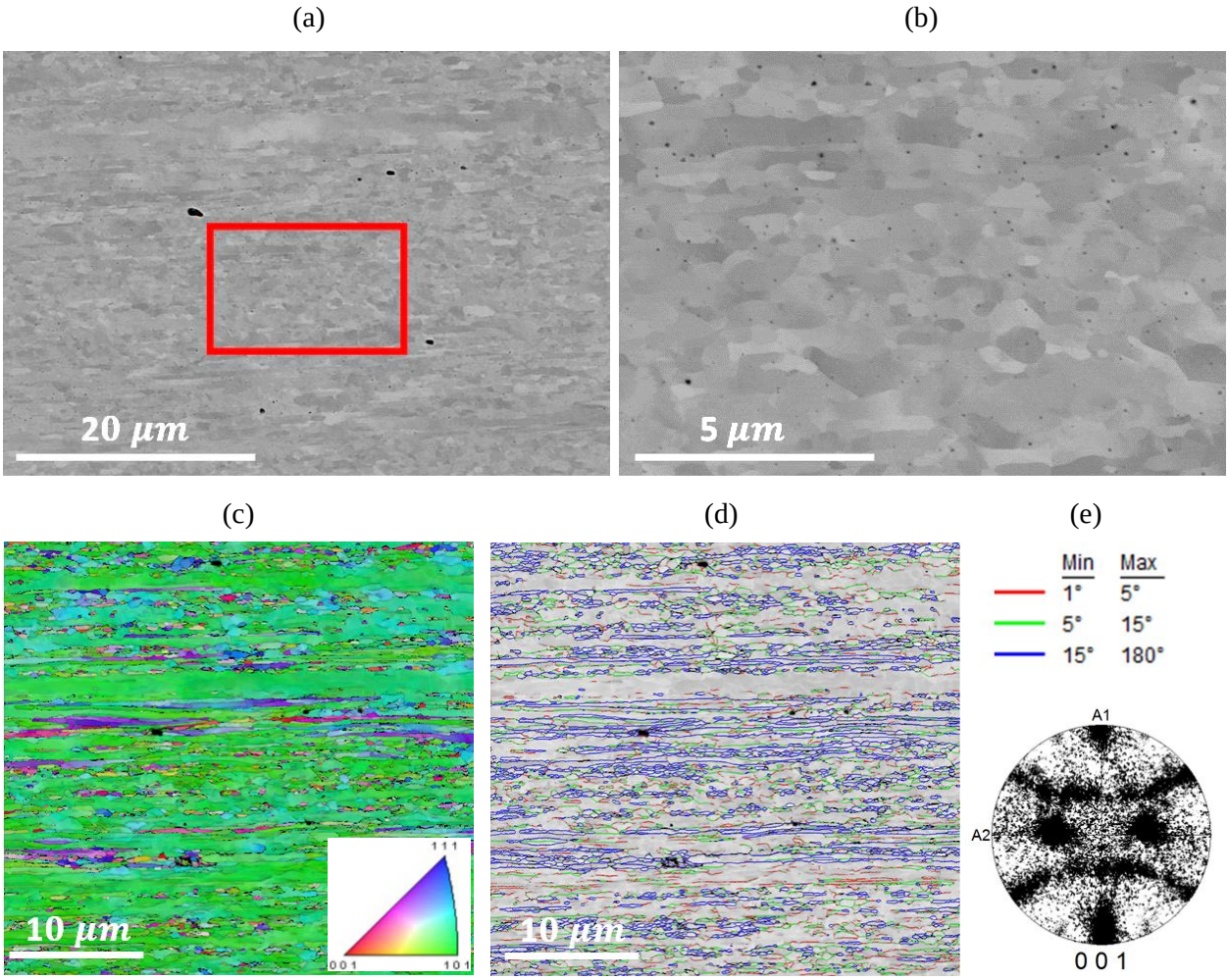


Figure 9. Showing the microstructure of the heat affected zone of the 1.0 mm thick plate of 14YWT in ROI #2 (Fig. 7). (a) and (b) BSE micrographs, (c) EBSD map and inverse pole figure (insert), (d) GIM map and (3) color indicator of GIM angles (top) and {001} pole figure (bottom).

Figure 10 shows the microstructure on the advancing side of the butt joint produced by FSW in the 1.0 mm thick plate of 14YWT, which is from ROI #3 (Fig. 7). The BSE micrographs observed in Figures 10a and 10b indicated that a considerable amount of porosity formed in the microstructure during FSW. The texture of the grains present in the butt joint on the advancing side is shown in Figures 10c, 10d and 10e. The EBSD map (Fig. 10c) showed the grains had coarsened and possessed a balance in orientations between the 3 poles {001}, {101} and {111}. The <001> pole figure (bottom in Fig. 10e) is consistent with many grains having multiple orientations between the 3 poles, but that there was an alignment of grains with {111} and {121} orientations. The GIM map of the microstructure shown in Figure 10d along with the color index of GIM angles shown in Figure 10e (top). The GIM map showed that most of the grains observed in the EBSD map (Fig. 10c) consisted of misorientation angles of 5º-15º (green) and >15º (blue) with effectively no grains having misorientation angles <5º (red). The GIM map indicated that the grain size determined by the high misorientation angles was increased in the butt joint by FSW. These results indicated that the highly anisotropic grain structure of the 1.0 mm thick plate of 14YWT completely recrystallized into coarser size grains with random texture due to the combination of high temperatures and severe deformations that occurred in the microstructure of the butt joint by FSW.

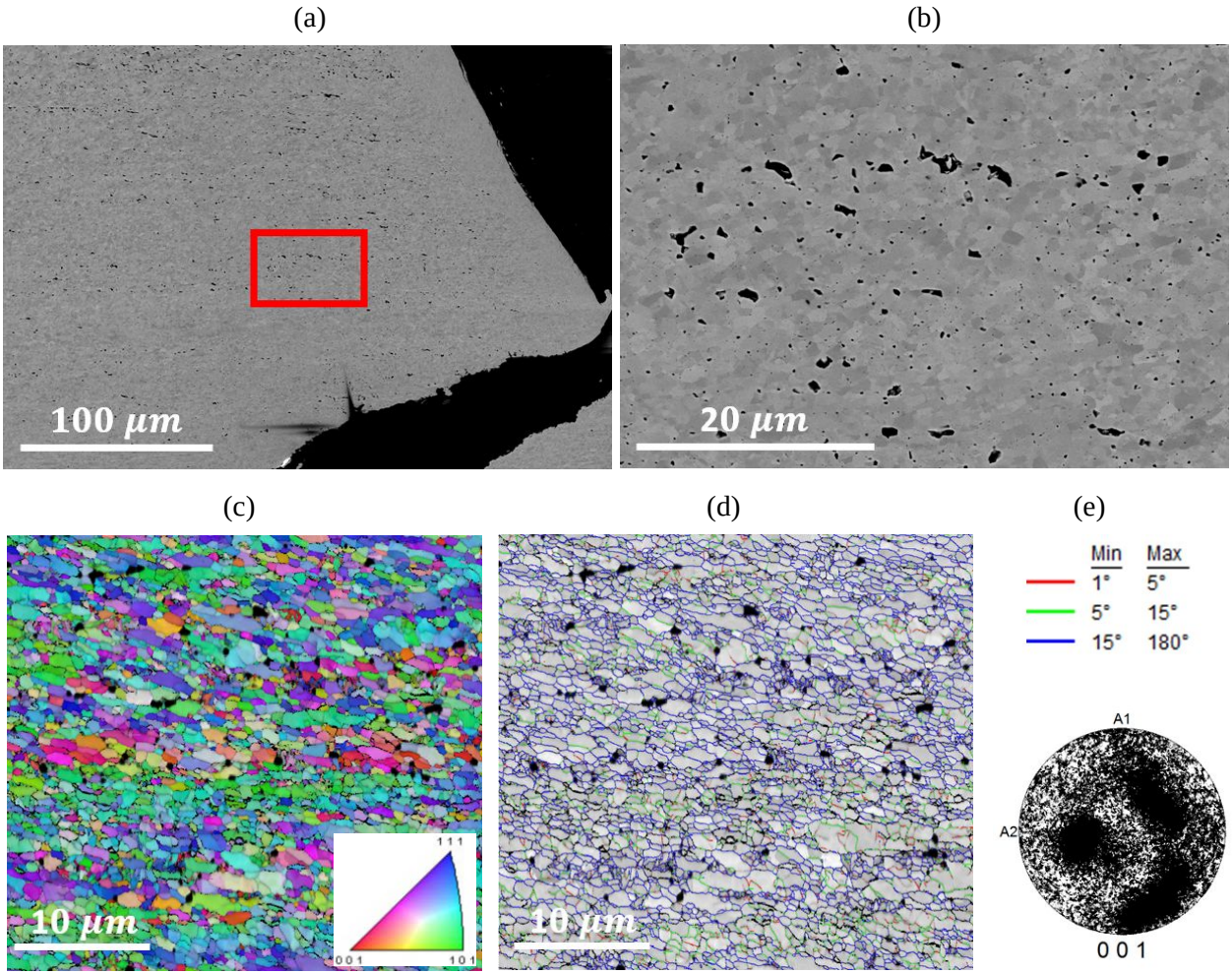


Figure 10. Showing the microstructure on the advancing side of the butt joint produced by FSW in the 1.0 mm thick plate of 14YWT in ROI #3 (Fig. 7). (a) and (b) BSE micrographs, (c) EBSD map and inverse pole figure (insert), (d) GIM map and (3) color indicator of GIM angles (top) and {001} pole figure (bottom).

Figure 11 shows the microstructure on the retreating side of the butt joint produced by FSW in the 1.0 mm thick plate of 14YWT from ROI #4 (Fig. 7). The BSE micrograph observed in Figures 11a shows two large pores and a distribution of smaller pores throughout the microstructure of the butt joint on the retreating side. Figure 11b shows an auto-grain map from EBSD with colors representing different grains. Most of the grains observed in the auto-grain map are elongated in a common direction that points to the upper-right corner of the micrographs. This observation implies that deformation and plastic flow of the grains occurred along this orientation in the butt joint on the retreating side during FSW. The EBSD and GIM maps shown in Figures 11c and 11d, respectively indicated that the microstructure in this region of the butt joint was more complex than that on the advancing size of the butt joint (Fig. 10). The EBSD map indicated that the grains were increased in size and randomly oriented between the 3 poles {001}, {101} and {111}. However, the grains observed in the EBSD map were not as prominent as those observed by EBSD on the advancing side of the butt joint (Fig. 10c). This observation is better understood by examining the GIM map (Fig. 11d). Most of the larger deformed grains were surrounded by grains with high misorientation angles of >15º (blue), although several horizontal bands of grains were present below the two pores composed of misorientation angles of <5º (red) and between 5º-15º (green). Another distinguishing feature of the GIM map were numerous small pockets of grains with low misorientations of <5º (red) that were mostly distributed in the microstructure containing grains with high misorientation angles of >15º (blue).

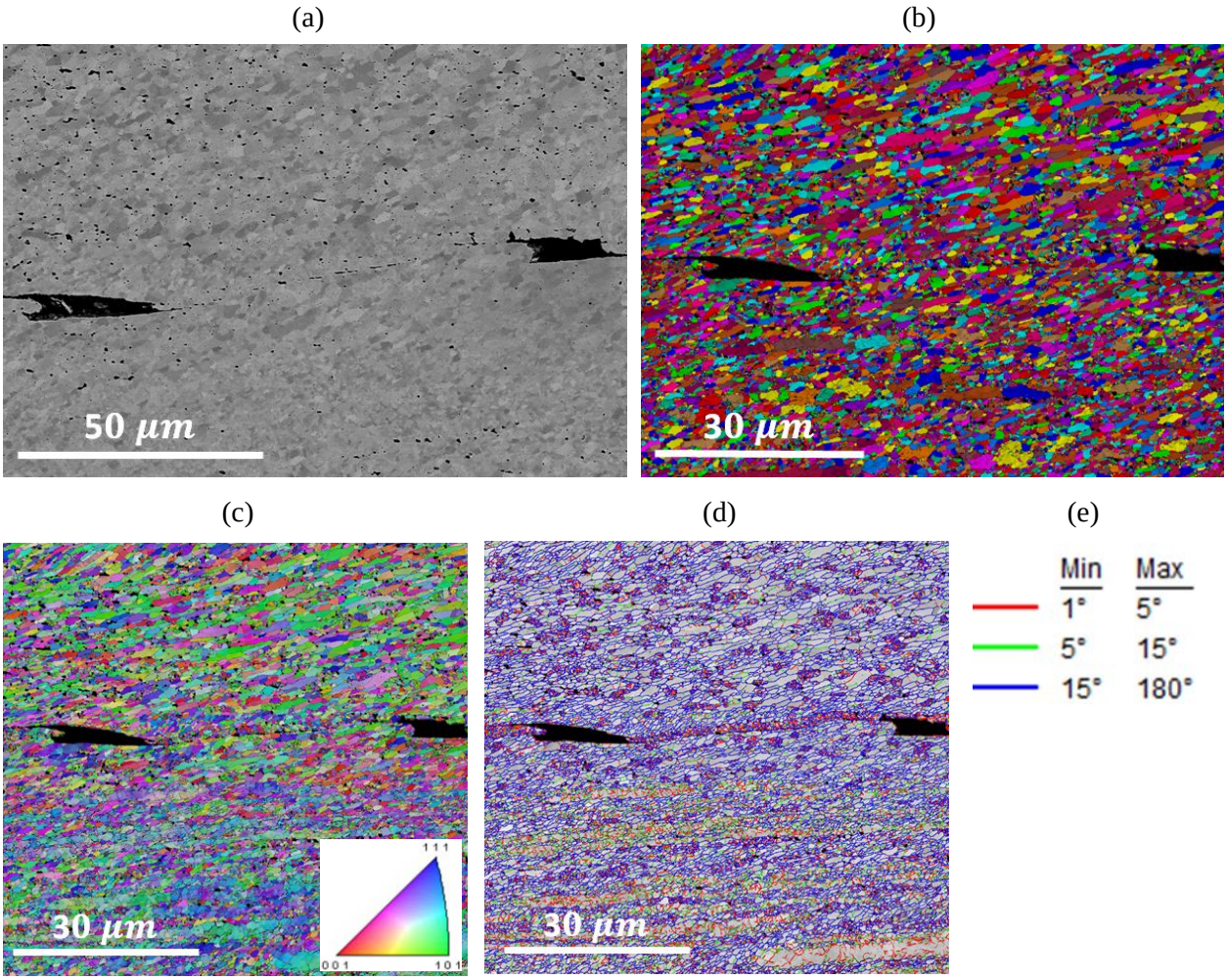


Figure 11. Showing the microstructure on the retreating side of the butt joint produced by FSW in the 1.0 mm thick plate of 14YWT in ROI #4 (Fig. 7). (a) and (b) BSE micrographs, (c) EBSD map and inverse pole figure (insert), (d) GIM map and (3) color indicator of GIM angles (top) and {001} pole figure (bottom).

In the GIM map that was shown in Figure 11d, a line of grains with low misorientation angles of <5º (red) were distributed between the two large pores along with numerous small pockets of grains with similarly low misorientation angles. A GIM map and BSE micrographs of this region obtained at higher magnification are shown in Figure 12. The red rectangular box observed on the GIM map (Fig. 12a) represents the region of the microstructure that is observed in the BSE micrograph (Fig. 12b), which also shows a red rectangular box that is observed in the BSE micrograph (Fig. 12c) obtained at higher magnification. At the higher magnification, the BSE micrograph had a resolution that was capable of resolving particle sizes >20 nm diameter. In Figure 12b, the grains are clearly defined in the upper left and lower right portions of the BSE micrograph and not so well defined in the central region. At higher magnification of the central region, the BSE micrograph shows sub-grain structures with grains. Correlating this observation with the GIM map (Fig. 12a), shows consistency between the sub-grain structure observed by BSE with the areas representing grains with low misorientation angles of <5º (red). These results indicate that both recrystallization and recovery mechanisms occurred in the grains that were located on the retreating side of the butt joint.

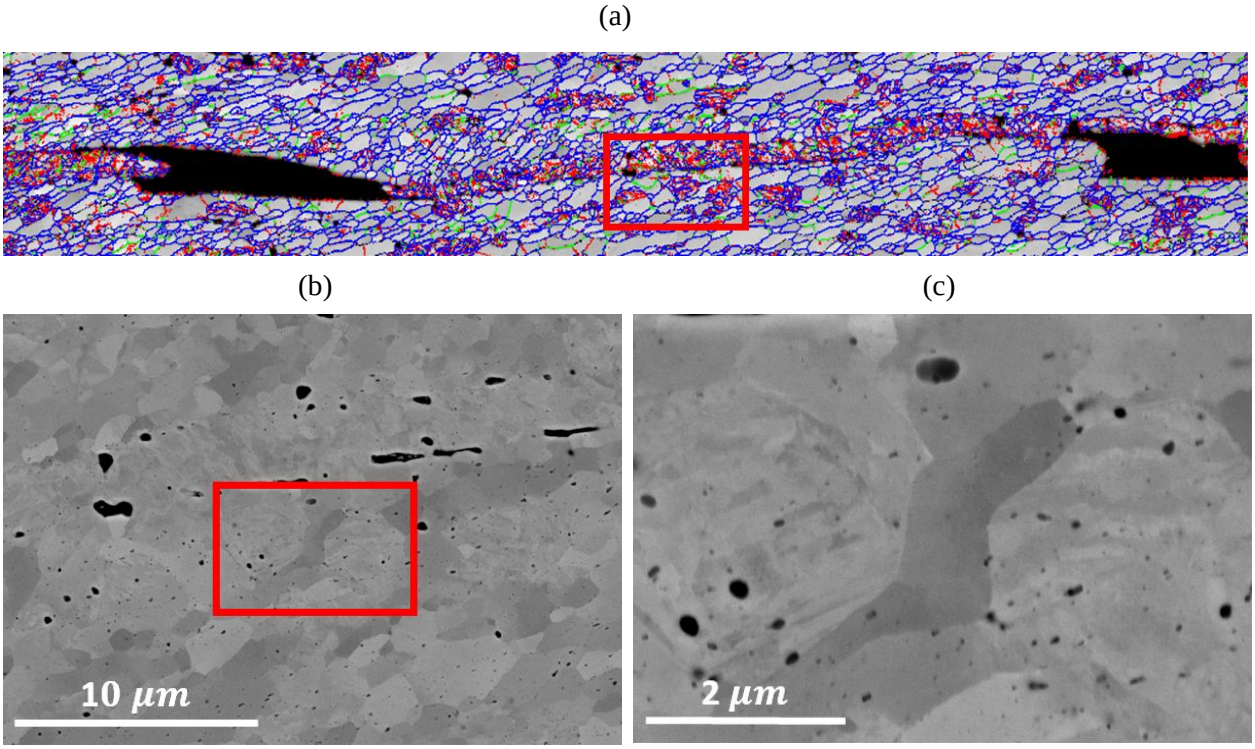


Figure 12. Showing the grain structure between two large pores observed on the retreating side of the butt joint produced by FSW in the 1.0 mm thick plate of 14YWT in ROI #4 (Fig. 7). (a) GIM map with ROI, (b) BSE micrograph of the ROI in the GIM map and (c) BSE micrograph at high magnification of the ROI observed in the BSE micrograph in (b).

## 4. SUMMARY

Friction stir welding using a modified tool pin produced a butt joint between two 1.0 mm thick plates of 14YWT, which was very challenging to achieve. The tool pin did not fully penetrate the butt joint resulting in a small but blunt notch between adjacent thin plates on the bottom surface of the butt joint. The weld zone showed good microstructure mixing with some flashing mostly on the retreating side that suggested excess heat input by friction between the traveling and spinning tool pin and thin plates of 14YWT. A bend occurred in the joined thin plate sample after the FSW run completed and the clamping was released. The peak displacement of the bend occurred along the center line of the butt joint was most likely caused by residual stresses that formed during FSW.

Neutron diffraction experiments were performed on the bent sample of 14YWT to measure the residual stresses in the butt joint on the HB-2B beam line at the Neutron Residual Stress Facility at HFIR. This research was associated with the ORNL Neutron Science User proposal (IPTS-19909.1) that was awarded beam time in January 2018. Unfortunately, low neutron scattering to background noise ratio was encountered during data acquisition that permitted measurement of lattice strains in two of three directions (ED, RD and ND) in the sample, but were not sufficient for determining the residual stresses in the butt joint. The low neutron scattering signal was due the uneven surface of the butt joint coupled with the reduction in thickness to ~0.7 mm on the advancing side of the butt joint from FSW. However, the residual stresses of four rolled plates of 14YWT were calculated from the lattice strain data obtained in the FY17 ORNL Neutron Science User proposal (IPTS-18043.1) and plotted in 2-D color contour maps for the extrusion (ED), rolling (RD) and normal (ND) directions. The results showed variations in the magnitude and spatial position of residual stresses in the microstructure of the four plates. The magnitude in residual

stresses increased gradually with increasing rolling deformation for plates R1 (50%) to R2 (76%), followed by larger increases in R3 (89%) and R4 (95%) in the ED and RD directions. The maximum peaks in residual stresses for the R4 plate was ~710-730 MPa in the ED and RD orientations. The residual stresses in ND were below ~300 MPa for each of the 4 rolled plates, with a maximum residual stress in R4 plate of ~400 MPa. These results indicated that significant residual stresses representing ~57% of the yield stress of 14YWT (SM13) had accumulated in the 14YWT plate after hot rolling to the 1 mm thickness, which was used in the FSW experiments.

The microstructure analysis of the 1.0 mm thick plate of 14YWT containing the butt joint produced by FSW revealed significant changes in the grain structure and texture between the unaffected zone (UZ) of the rolled plate and the butt joint weld. In the UZ, the grains were severely elongated due to the 95% rolling deformation having mainly the {101} texture component in the extrusion direction and two predominant grain misorientations consisting of small misorientations of <5º between the highly elongated grains and large misorientations of >15º in pockets of small grains. The pockets of small grains most likely formed by dynamic recrystallization processes during rolling of the plate at 1000ºC. A heat affected zone (HAZ) was observed adjacent to the butt joint. The grains in the HAZ had coarsened due to excess heat input during FSZ while the texture of the grains was mostly {101}, which was similar to the UZ, and most of the grains were separated by large misorientations of >15º. The microstructure of the advancing and retreating sides of the butt joint were characterized. In both regions, the pores were distributed in the microstructure and the grains increased in size showing mostly isotropic morphologies. The grains in both regions had random orientations between the 3 poles {001}, {101} and {111}. The main difference in the texture between the advancing side and retreating side was with the misorientation angles of neighboring grains. In the advancing side, most of the grains had misorientation angles of >5º indicating recrystallization occurred resulting in the coarser size of the grains and the random texture. On the retreating side the EBSD maps of the grains indicated that two regions existed: areas containing larger grains showed high misorientation angles of >15º and areas appearing as bands of grains were composed of grains with misorientation angles of <5º and between 5º-15º. Another distinguishing feature of the texture were numerous small pockets of grains with low misorientations of <5º that were mostly distributed in the microstructure containing grains with high misorientation angles of >15º. It was determined that the grains associated with low misorientation angles contained sub-grain structures, which was consistent with both recrystallization and recovery mechanisms for grains located on the retreating side of the butt joint. These results demonstrate the complex microstructure that evolves in the microstructure of 14YWT resulting from the input of high temperatures and severe deformations during FSW.

## REFERENCES


[1] Y. Gan, K. Mo, D. Yun, D.T. Hoelzer, Y. Miao, Z. Liu, K-C. Lan, J-S. Park, J. Almer, T. Chen and H. Zhao, Materials Science & Engineering A, 692 (2017) 53-61.

[2] Y.G. Kim, H. Fujii, T. Tsumura, T. Komazaki and K. Nakata, Materials Science & Engineering A, 415 (2006) 250-254.

[3] S. Pal, M.E. Alam, S.A. Maloy, D.T. Hoelzer and G.R. Odette, Acta Materialia, 152 (2018) 338-357.